

Optical properties of quasi-tetragonal BiFeO₃ thin films

P. Chen, N. J. Podraza, X. S. Xu, A. Melville, E. Vlahos, V. Gopalan, R. Ramesh, D. G. Schlom, and J. L. Musfeldt

Citation: *Applied Physics Letters* **96**, 131907 (2010); doi: 10.1063/1.3364133

View online: <http://dx.doi.org/10.1063/1.3364133>

View Table of Contents: <http://scitation.aip.org/content/aip/journal/apl/96/13?ver=pdfcov>

Published by the **AIP Publishing**

Articles you may be interested in

[Optical properties of epitaxial BiFeO₃ thin films grown on LaAlO₃](#)

Appl. Phys. Lett. **106**, 012908 (2015); 10.1063/1.4905443

[High-frequency electromagnetic properties of epitaxial Bi₂FeCrO₆ thin films grown by pulsed laser deposition](#)

Appl. Phys. Lett. **99**, 183505 (2011); 10.1063/1.3657528

[Optical properties of an epitaxial Na_{0.5}Bi_{0.5}TiO₃ thin film grown by laser ablation: Experimental approach and density functional theory calculations](#)

J. Appl. Phys. **107**, 104107 (2010); 10.1063/1.3400095

[Growth, crystal structure, and properties of epitaxial Bi₂ScO₃ thin films](#)

J. Appl. Phys. **104**, 044102 (2008); 10.1063/1.2964087

[Optical properties of \$\delta\$ -Bi₂O₃ thin films grown by reactive sputtering](#)

Appl. Phys. Lett. **87**, 231916 (2005); 10.1063/1.2136351

You don't still use this cell phone

or this computer

Why are you still using an AFM designed in the 80's?

It is time to upgrade your AFM

Minimum \$20,000 trade-in discount for purchases before August 31st

Asylum Research is today's technology leader in AFM

dropmyoldAFM@oxinst.com

OXFORD
INSTRUMENTS
The Business of Science®

Optical properties of quasi-tetragonal BiFeO₃ thin films

P. Chen,^{1,a)} N. J. Podraza,² X. S. Xu,^{1,b)} A. Melville,³ E. Vlahos,⁴ V. Gopalan,⁴ R. Ramesh,^{5,6} D. G. Schlom,³ and J. L. Musfeldt¹

¹Department of Chemistry, University of Tennessee, Knoxville, Tennessee 37996, USA

²Department of Electrical Engineering, Pennsylvania State University, University Park, Pennsylvania 16802, USA

³Department of Materials Science and Engineering, Cornell University, Ithaca, New York 14853-1501, USA

⁴Department of Materials Science and Engineering, Pennsylvania State University, University Park, Pennsylvania 16802, USA

⁵Department of Materials Science and Engineering, University of California-Berkeley, Berkeley, California 94720, USA

⁶Materials Science Division, Lawrence Berkeley National Laboratory, Berkeley, California 94720, USA

(Received 2 February 2010; accepted 23 February 2010; published online 1 April 2010)

Optical transmission spectroscopy and spectroscopic ellipsometry were used to extract the optical properties of an epitaxially grown quasi-tetragonal BiFeO₃ thin film in the near infrared to near ultraviolet range. The absorption spectrum is overall blue shifted compared with that of rhombohedral BiFeO₃, with an absorption onset near 2.25 eV, a direct 3.1 eV band gap, and charge transfer excitations that are ~0.4 eV higher than those of the rhombohedral counterpart. We interpret these results in terms of structural strain and local symmetry breaking. © 2010 American Institute of Physics. [doi:10.1063/1.3364133]

The physical properties of polar oxides are of foundational importance for investigations of coupling in functional materials. This is because the rich tunability in these systems arises from the interplay between charge, structure, and magnetism. In thin film oxides, strain is well known to modify hybridization and bonding and, as a consequence, the bulk properties.¹⁻³ It can also stabilize nonequilibrium (metastable) phases. In this work, we focus on bismuth ferrite, the only known single phase room temperature multiferroic. BiFeO₃ displays many exotic properties including magnetoelectric coupling,^{4,5} a large remanent polarization,^{6,7} and photovoltaic current,⁸ and it is already incorporated in polar oxide-based solar cells and actuators.^{9,10} In both applications, the different phases of the parent material play a vital role, either to achieve better match with the solar spectrum or to define a morphotropic phase boundary. In this work, we investigate the optical properties of quasi-tetragonal¹¹ BiFeO₃, a phase stabilized by compressive strain.¹⁰

Bulk BiFeO₃ is ferroelectric ($T_C \sim 1100$ K) and antiferromagnetic ($T_N \sim 640$ K) at 300 K. The structure is that of a rhombohedrally distorted perovskite¹² belonging to the $R3c$ space group. Each Fe³⁺ center is coordinated by six O²⁻ ions [Fig. 1(a)], although the distortion along [111] yields a quasi-octahedral arrangement. A slight tetragonal distortion reduces the space group to $P4mm$ (Ref. 14) and modifies the overall perovskite structure so that the local Fe³⁺ environment is quasi-square pyramidal [Fig. 1(b)]. Theoretical calculations predict an unusually large tetragonality ratio for this system.^{10,14,15} In practice, the nonequilibrium tetragonal phase can be stabilized by compressive strain, and epitaxial films with different c/a ratios have been reported.^{10,15,16}

In order to investigate the impact of strain on the charge excitations of a model polar oxide, we measured the optical properties of tetragonal BiFeO₃ and compared the results

with rhombohedral films¹⁷⁻²⁰ and recent first principles electronic structure calculations.^{14,15} We find that the optical response of tetragonal BiFeO₃ is overall blue shifted, with an absorption onset near 2.25 eV and a direct band gap and charge transfer excitations that are ~0.4 eV higher than those of the rhombohedral material. These results can be understood in terms of symmetry breaking and local structure strain.

A series of tetragonal BiFeO₃ films with thicknesses between 23 and 38 nm were deposited on (110) YAlO₃ substrates using conventional and laser molecular-beam epitaxy.¹⁰ The pure tetragonal phase with small monoclinic distortion is stabilized by the large epitaxial stain due to lattice mismatch with the substrate.¹⁰ X-ray results show only substrate and film peaks, and these films have a c/a ratio of 1.27. Rocking curves show partial relaxation but with a full width at half max that is virtually the same as the substrate. We employed both optical transmission spectroscopy and spectroscopic ellipsometry to elucidate the optical properties of this nonequilibrium phase. A combination of techniques was employed due to the challenges inherent in a thin film measurement. These include (i) important reflectance contributions in a normal-incidence transmittance measurement when the absorption coefficient is low and (ii) surface rough-

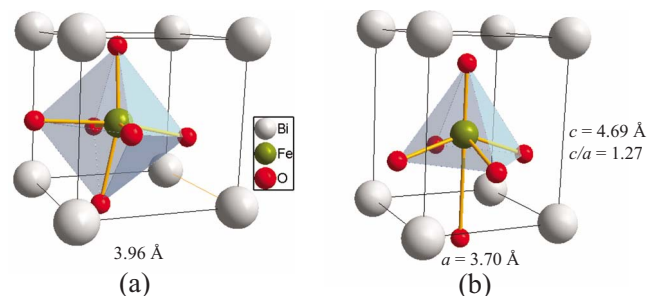


FIG. 1. (Color online) Schematic view of the local structure around the Fe³⁺ center of (a) rhombohedral (Ref. 13) and (b) tetragonal (Ref. 14) BiFeO₃.

^{a)}Electronic mail: pchen@ion.chem.utk.edu.

^{b)}Present address: Oak Ridge National Laboratories, Oak Ridge, TN.

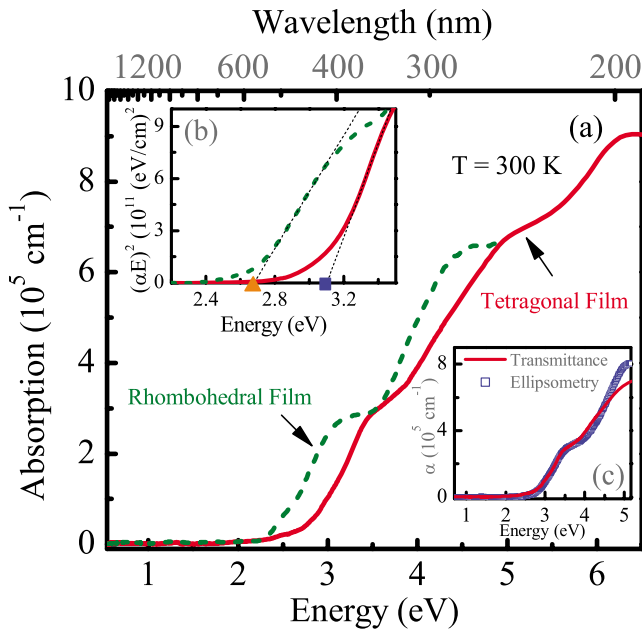


FIG. 2. (Color online) (a) Absorption coefficient of tetragonal BiFeO₃ compared with that of the rhombohedral system (Ref. 17). (b) Direct band gap analysis of both materials. The triangle marks the 2.67 ± 0.02 eV charge gap of the rhombohedral film whereas the square marks the 3.10 ± 0.02 eV charge gap of tetragonal BiFeO₃. (c) $\alpha(E)$ obtained by optical transmittance compares well with that obtained by ellipsometry.

ness sensitivity and the difficulty in characterizing low absorption coefficients via ellipsometry.^{21,22} Room temperature transmittance and reflectance spectra were collected using a Perkin-Elmer Lambda-900 spectrometer (3000–190 nm; 0.41–6.53 eV). We calculated the absorption coefficient $\alpha(E)$ from combined transmittance and reflectance measurements.²³ Ellipsometric spectra (in Δ, ψ) were extracted at four angles of incidence, $\Theta = 50^\circ, 60^\circ, 70^\circ,$ and 80° , using a variable-angle dual rotating-compensator multi-channel spectroscopic ellipsometer²⁴ over a spectral range from 0.75 to 5.15 eV. $\alpha(E)$ was also determined from spectroscopic ellipsometry analysis and compared with the complementary data obtained from optical transmittance.

Figure 2(a) displays the 300 K absorption spectrum of the tetragonal BiFeO₃ film compared with that of the rhombohedral analog.¹⁷ We assigned the observed excitations based on recent first-principles calculations.^{14,15,25} Although the overall absorption profiles are similar, the familiar 3.2 and 4.5 eV electronic excitations of the rhombohedral material, assigned as minority channel dipole-allowed charge transfer features,^{17,18,25} are blue shifted by ~ 0.4 eV in tetragonal BiFeO₃. The blue shift of these strongly hybridized O *p* to Fe *d* excitations is a consequence of the strained nature of the nonequilibrium tetragonal phase. The quasi-tetragonal film displays an additional electronic feature centered at ~ 6.2 eV that we assign as a strongly hybridized majority channel O *p*+Fe *d* \rightarrow Bi *p* state excitation. The direct band gap is extracted by a linear extrapolation of an $(\alpha \cdot E)^2$ versus *E* plot to zero [Fig. 2(b)].²¹ We find the band gap in tetragonal BiFeO₃ to be 3.10 ± 0.02 eV, ~ 0.4 eV larger than that in rhombohedral BiFeO₃ (2.67 ± 0.02 eV). This result is different from the recent theoretical calculations^{14,15} that predict a smaller band gap in tetragonal BiFeO₃. The 2.5 eV sub band gap absorption feature in the rhombohedral system¹⁷ is also present in the tetragonal ma-

TABLE I. Dielectric function parameters for rhombohedral and tetragonal BiFeO₃. All Tauc-Lorentz (TL) oscillators (Ref. 29) share a common Tauc gap $E_g = 2.14$, $\epsilon_\infty = 2.24$ for the rhombohedral film and $E_g = 2.30$, $\epsilon_\infty = 2.49$ for the tetragonal film, where ϵ_∞ is the high frequency permittivity a constant additive term to ϵ_1 . SO, E₀, A, and Γ are, respectively, the Sellmeier oscillator (Ref. 30), resonance energy, amplitude, and broadening. All parameters are in units of energy (electron volts).

Oscillator	Rhombohedral <i>R3c</i> ^a			Tetragonal <i>P4mm</i>		
	E ₀	A	Γ	E ₀	A	Γ
TL ₁	2.39	9.54	0.31	3.01	1.05	0.24
TL ₂	2.97	36.10	0.70	3.37	33.50	0.98
TL ₃	4.19	44.03	1.63	4.91	47.03	1.77
TL ₄ /SO	6.15	38.66	3.47	6.50	6.04	0

^aReference 20.

terial. This feature contributes to the onset of optical absorption at ~ 2.25 eV and is probably a collective excitation.²⁶

The experimental ellipsometric spectra were fit to a parameterized optical and structural model using a least-squares regression analysis with an unweighted error function²⁷ in order to extract the complex dielectric function spectra and microstructural parameters. The latter include bulk film and surface roughness thicknesses. The optical properties of the surface roughness layer were represented by the Bruggeman effective medium approximation consisting of fractions of bulk material and void.²⁸ The fitting parameters of both materials are given in Table I. The average unweighted error function obtained from the least-squares regression fitting is sufficiently low with a value of 6.4×10^{-3} , indicating that the fit using this model is reasonable. Dielectric functions were extracted by numerical inversion from each (Δ, ψ) spectra using the bulk film and surface roughness thicknesses determined from the parameterized fit. Figure 3 displays $\epsilon_1(E)$ and $\epsilon_2(E)$ for the quasi-tetragonal BiFeO₃ film compared to similar results on the rhombohedral material.¹⁹ Tetragonal BiFeO₃ exhibits higher energy charge transfer excitations that are also broadened compared with the rhombohedral phase, a result that is overall consistent with the absorption spectra in Fig. 2(c).

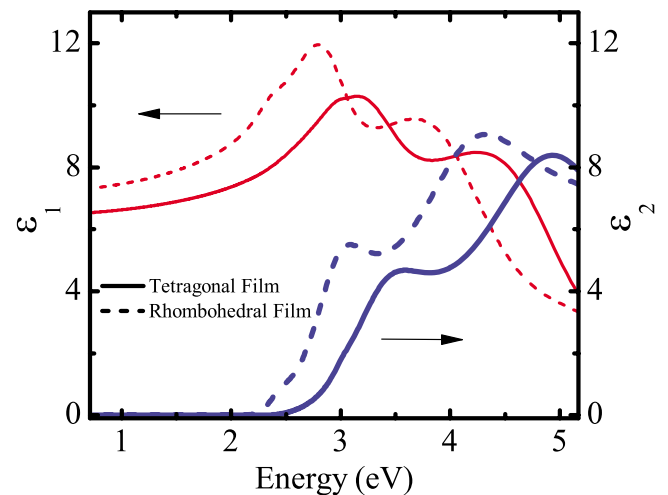


FIG. 3. (Color online) Complex dielectric function spectra ($\epsilon = \epsilon_1 + i\epsilon_2$) vs photon energy (*E*) obtained for tetragonal BiFeO₃ (solid line). $\epsilon_1(E)$ and $\epsilon_2(E)$ of rhombohedral BiFeO₃ (dashed line) are shown for comparison (Ref. 19).

We can also compare the optical properties of tetragonal BiFeO₃ with a local structure analysis [Fig. 1], simple crystal field theory, and first principles electronic structure calculations.^{14,15} We begin by considering the FeO₆ structure in rhombohedral BiFeO₃ as an ideal octahedron. It is well-known that, in an octahedral crystal field, the 3*d* orbital states split into *t*_{2*g*} and *e*_g levels. Strain has important consequences for the local structure. In tetragonal BiFeO₃, one of the Fe–O axial distances increases to ~2.80 Å, and the Fe–O equatorial bond lengths are reduced to ~1.93 Å.¹⁴ These modifications split the *t*_{2*g*} states into a doubly-degenerate pair (*d*_{*xz*}, *d*_{*yz*}) and a singly-degenerate *d*_{*xy*} level, and the *e*_g states break symmetry to yield a lower energy *d*_{*z*²} state and a higher energy *d*_{*x*²–*y*²} level. The net effect is to move the empty Fe³⁺ 3*d* states closer to the occupied ones. Band structure calculations^{14,15} confirm this trend, predicting that the unoccupied Fe³⁺ 3*d* states broaden and move closer to the Fermi level in the quasi-tetragonal system. At the same time, the calculations predict that the O²⁻ 2*p* states move further away from the Fermi level.¹⁴ Together, these competing density of states shifts define the predicted charge gap. In other words, this is a joint density of states effect. Based upon our measurement of a larger band gap in quasi-tetragonal BiFeO₃ compared to that in the rhombohedral analog, the calculations either overestimate the strain-induced shift in the Fe³⁺ 3*d* states or underestimate the shift of the O²⁻ 2*p* states.

To summarize, both optical transmission spectroscopy and spectroscopic ellipsometry were used to reveal the optical properties of quasi-tetragonal BiFeO₃. Due to the structure strain and symmetry breaking induced distortions of the local Fe³⁺ crystal field and shifts in the O 2*p* states, the band gap and charge transfer excitations are blue shifted compared with those in the rhombohedral material. Although compressive strain stabilizes a non-equilibrium phase, its optical properties are unfortunately a less attractive match with the solar spectrum. On the other hand, an applied electric field can drive a morphotropic phase transition,¹⁰ a result that may allow the development of an electro-optic switch.

This work was supported by the U.S. DOE (Grant Nos. DE-FG02-01ER45885 at UT and DE-AC02-05CH1123 at Berkeley), NSF (Grant Nos. DMR-0820404 and DMR-0908718 at PSU and CU), and ARO (Grant No. W911NF-08-2-0032 at CU). We thank H. M. Tütüncü for useful discussions.

¹J. H. Haeni, P. Irvin, W. Chang, R. Uecker, P. Reiche, Y. L. Li, S. Choudhury, W. Tian, M. E. Hawley, B. Craigo, A. K. Tagantsev, X. Q. Pan, S. K. Streiffer, L. Q. Chen, S. W. Kirchoefer, J. Levy, and D. G. Schlom, *Nature (London)* **430**, 758 (2004).

²K. J. Choi, M. Biegalski, Y. L. Li, A. Sharan, J. Schubert, R. Uecker, P. Reiche, Y. B. Chen, X. Q. Pan, V. Gopalan, L.-Q. Chen, D. G. Schlom, and C. B. Eom, *Science* **306**, 1005 (2004).

³K. M. Rabe, *Curr. Opin. Solid State Mater. Sci.* **9**, 122 (2005).

⁴A. M. Kadomtseva, A. K. Zvezdin, Y. F. Popov, A. P. Pyatakov, and G. P. Vorob'ev, *JETP Lett.* **79**, 571 (2004).

⁵T. Zhao, A. Scholl, F. Zavaliche, K. Lee, M. Barry, A. Doran, M. P. Cruz,

Y. H. Chu, C. Ederer, N. A. Spaldin, R. R. Das, D. M. Kim, S. H. Baek, C. B. Eom, and R. Ramesh, *Nature Mater.* **5**, 823 (2006).

⁶H. W. Jang, S. H. Baek, D. Ortiz, C. M. Folkman, C. B. Eom, Y. H. Chu, P. Shafer, R. Ramesh, V. Vaithyanathan, and D. G. Schlom, *Appl. Phys. Lett.* **92**, 062910 (2008).

⁷J. Wang, J. B. Neaton, H. Zheng, V. Nagarajan, S. B. Ogale, B. Liu, D. Viehland, V. Vaithyanathan, D. G. Schlom, U. V. Waghmare, N. A. Spaldin, K. M. Rabe, M. Wuttig, and R. Ramesh, *Science* **299**, 1719 (2003).

⁸T. Choi, S. Lee, Y. J. Choi, V. Kiryukhin, and S.-W. Cheong, *Science* **324**, 63 (2009).

⁹S. Y. Yang, L. W. Martin, S. J. Byrnes, T. E. Conry, S. R. Basu, D. Parani, L. Teichert, J. Ihlefeld, C. Adamo, A. Melville, Y.-H. Chu, C.-H. Yang, J. L. Musfeldt, D. G. Schlom, J. W. Ager III, and R. Ramesh, *Appl. Phys. Lett.* **95**, 062909 (2009).

¹⁰R. J. Zeches, M. D. Rossell, J. X. Zhang, A. J. Hatt, Q. He, C.-H. Yang, A. Kumar, C. H. Wang, A. Melville, C. Adamo, G. Sheng, Y.-H. Chu, J. F. Ihlefeld, R. Erni, C. Ederer, V. Gopalan, L. Q. Chen, D. G. Schlom, N. A. Spaldin, L. W. Martin, and R. Ramesh, *Science* **326**, 977 (2009).

¹¹The true symmetry of the strain-stabilized phase that is the subject of this paper is monoclinic, but it's a different phase than the isostructural (also monoclinic) distorted rhombohedral BiFeO₃ phase that has been widely studied in thin film form (Refs. 4–9 and 17–20). As one is a slight monoclinic distortion from tetragonal BiFeO₃ and the other a slight monoclinic distortion from rhombohedral BiFeO₃ (Ref. 10), we refer to these two distinct phases as simply tetragonal and rhombohedral BiFeO₃, which is an oversimplification.

¹²P. Fischer, M. Polomska, I. Sosnowska, and M. Szymanski, *J. Phys. C* **13**, 1931 (1980).

¹³F. Kubel and H. Schmid, *Acta Crystallogr., Sect. B: Struct. Sci.* **46**, 698 (1990).

¹⁴H. M. Tütüncü and G. P. Srivastava, *Phys. Rev. B* **78**, 235209 (2008).

¹⁵D. Ricinschi, K.-Y. Yun, and M. Okuyama, *J. Phys.: Condens. Matter* **18**, L97 (2006).

¹⁶K. Y. Yun, D. Ricinschi, T. Kanashima, M. Noda, and M. Okuyama, *Jpn. J. Appl. Phys., Part 2* **43**, L647 (2004).

¹⁷S. R. Basu, L. W. Martin, Y. H. Chu, M. Gajek, R. Ramesh, R. C. Rai, X. Xu, and J. L. Musfeldt, *Appl. Phys. Lett.* **92**, 091905 (2008).

¹⁸X. S. Xu, T. V. Brinzari, S. Lee, Y. H. Chu, L. W. Martin, A. Kumar, S. McGill, R. C. Rai, R. Ramesh, V. Gopalan, S.-W. Cheong, and J. L. Musfeldt, *Phys. Rev. B* **79**, 134425 (2009).

¹⁹J. F. Ihlefeld, N. J. Podraza, Z. K. Liu, R. C. Rai, X. Xu, T. Heeg, Y. B. Chen, J. Li, R. W. Collins, J. L. Musfeldt, X. Q. Pan, J. Schubert, R. Ramesh, and D. G. Schlom, *Appl. Phys. Lett.* **92**, 142908 (2008).

²⁰A. Kumar, R. C. Rai, N. J. Podraza, S. Denev, M. Ramirez, Y. H. Chu, L. W. Martin, J. Ihlefeld, T. Heeg, J. Schubert, D. G. Schlom, J. Orenstein, R. Ramesh, R. W. Collins, J. L. Musfeldt, and V. Gopalan, *Appl. Phys. Lett.* **92**, 121915 (2008).

²¹F. Wooten, *Optical Properties of Solids* (Academic, New York, 1972).

²²H. Fujiwara, *Spectroscopic Ellipsometry: Principles and Applications* (Wiley, West Sussex, England, 2007).

²³M. Tinkham, in *Far Infrared Properties of Solids*, edited by S. S. Mitra and S. Nudelman (Plenum, New York, 1970), p. 233.

²⁴C. Chen, I. An, G. M. Ferreira, N. J. Podraza, J. A. Zapien, and R. W. Collins, *Thin Solid Films* **455-456**, 14 (2004).

²⁵J. B. Neaton, C. Ederer, U. V. Waghmare, N. A. Spaldin, and K. M. Rabe, *Phys. Rev. B* **71**, 014113 (2005).

²⁶X. S. Xu, J. H. Lee, J. Ihlefeld, A. Kumar, R. Ramesh, V. Gopalan, D. G. Schlom, and J. L. Musfeldt, "Tunable band gap in Bi(Fe_{1-x}Mn_x)O₃ films" (unpublished).

²⁷Y. Cong, I. An, K. Vadam, and R. W. Collins, *Appl. Opt.* **30**, 2692 (1991).

²⁸H. Fujiwara, J. Koh, P. I. Rovira, and R. W. Collins, *Phys. Rev. B* **61**, 10832 (2000).

²⁹G. E. Jellison, Jr. and F. A. Modine, *Appl. Phys. Lett.* **69**, 371 (1996).

³⁰R. W. Collins and A. S. Ferlauto, in *Handbook of Ellipsometry*, edited by H. G. Tompkins and E. A. Irene (William Andrew, Norwich, NY, 2005), pp. 125–129.